Meissner Levitated Magnetic Microparticle

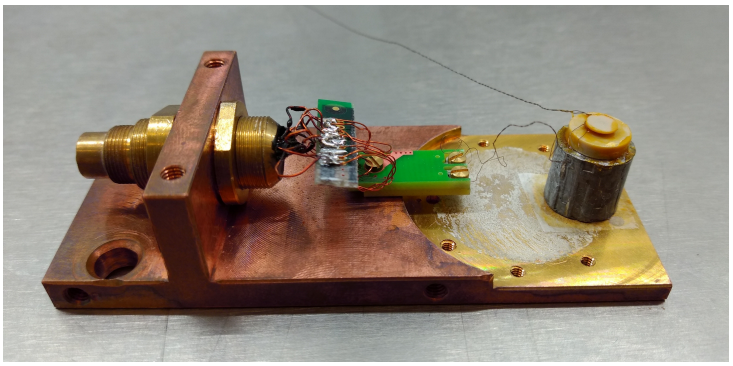

THESIS

submitted in partial fulfillment of the
requirements for the degree of

MASTER OF SCIENCE
in
PHYSICS

Author :	Jean-Paul van Soest
Student ID :	1650939
Supervisor :	Prof.dr.ir. Tjerk H. Oosterkamp
	Tim M. Fuchs, MSc
2^{nd} corrector :	Dr. Wolfgang Löffler

Leiden, the Netherlands, August 27, 2020

Meissner Levitated Magnetic Microparticle

Jean-Paul van Soest

Huygens-Kamerlingh Onnes Laboratory, Leiden University
Niels Bohrweg 2, 2333 CA Leiden, the Netherlands

August 27, 2020

Abstract

Well isolated mechanical systems have the potential to be developed into systems for magnetic, accelerometric and gravitational sensing, as well as to investigate the limits of quantum theory. This holds especially for mechanical resonators which consist of levitated nano- and microparticles, since an advantage of this type of system is the lack of clamping losses, potentially resulting in an extremely low energy dissipation. Here, a mechanical resonator is presented, where a magnetic microparticle is levitated in a cylindrical trap of a type I superconductor. SQUID detection has been used to measure the vibrational modes of the particle. The damping factors of the resonator have been analytically calculated, resulting in an expected quality factor Q of 10^{11}. The coupling and energy of the six translational and rotational rigid body modes of the particle have been simulated, based on analytical approximations. Experimentally, a resonance is detected with a damping time of 47 seconds and a Q of $2.2 \cdot 10^4$. These are promising first results, since this difference in damping and Q factor can be explained as the Earth's magnetic field was trapped inside the experiment. With these complications resolved, an extremely sensitive micromechanical resonator can be developed. This opens a new road in the investigation of the boundary between the quantum and classical regime and gravitational research.

Contents

Chapter 1

Introduction

1.1 Background

Ever since the early days of quantum mechanics people have been questioning to what extent this theory can be applied. Generally, the point where this breaks down is due to the size, mass or complexity of a system. One class of systems, however, could possibly overcome this hurdle and has recently emerged in the investigation of the boundary between the quantum and the classical regime.

These systems are micromechanical resonators, which consist of a mesoscopic element which can be brought to its ground state. These resonators can be cooled down to mK temperatures in order to reduce the internal energy of the system and its thermal noise. Here, they could occupy a superposition of quantum mechanical states, which is relatively simple to investigate.

To date, many types of mechanically resonating systems have been developed. These include, among others, nanobeams and membranes.[1–3] The efficiency of a system, and its detachment from its surroundings, is measured by its quality (Q) factor, which is related to the energy dissipation of the resonator and will be discussed in Chapter 2. State-of-the-art micromechanical resonators obtain a Q factor of $10^9 - 10^{10}$.[1, 4] These systems are, however, optimized for MHz and GHz frequencies. Also, they suffer from clamping losses as their leading term in energy dissipation. Therefore, it is becoming increasingly difficult to push these systems to higher Q factors, due to the intrinsic mechanical link to their surroundings.

Recently, a type of system has come up that does not have any clamping losses. The Oosterkamp group has developed what we call the *Lead Zeppelin*, where a superconducting microparticle is levitated in an anti-Helmholtz magnetic field.[5] Due to the small interaction with its surroundings the resonator has very little energy dissipation. A disadvantage, however, is the small magnetic coupling due to the weak magnetic field.

Vinante et al. have experimentally presented an opposite approach: a magnetic microparticle levitating in a superconducting well.[6] An advantage of this system is that only static magnetic fields are used. Thus, a feedback system is not needed in order to control the resonator.

1.2 Research

Vinante et al. achieved a Q factor of 10^7, which is promising for forthcoming experiments. Because this experiment is performed at a temperature of 4 K and a pressure of 10^{-4} mbar. This caused their leading cause of energy dissipation to be viscous drag. In this thesis, a similar experiment of a Meissner levitated magnetic microparticle is presented. SQUID-detection will be used to measure the movement of the particle, which causes very little energy dissipation and is the most noninvasive detection method. Since a temperature of 10 mK is obtained, the pressure in this experiment will be below 10^{-9} mbar. The viscous drag will therefore be smaller and it is expected that the leading energy dissipation will be caused by eddy currents instead of viscous drag. With this, a Q factor of 10^{11} is expected.

Several functioning samples have been developed, on which ringdown measurements have been performed. Here, the levitated particle is actively driven at its resonance frequency, after which the damping time τ has been measured. Also, a frequency shift has been observed for high amplitudes of the resonator, as will be discussed in Chapters 2 and 4.

An advantage of this system is that the micromechanical resonator can be designed to have any resonance frequency desired, including low frequencies on the order of 1 Hz. It could be developed for an extremely sensitive sensor for, for example, small magnetic fields or very precise acceleration measurements. A third, more fundamentally driven, impulse is to research the edge between quantum and classical mechanics. Finally, the resonator could be used in the research on gravitational effects. One

may study the gravity sourced by very small masses. With this, the gravitational constant could possibly be determined more accurately.

Chapter 2

Theory

2.1 The harmonic oscillator

In nature almost all systems that are brought out of equilibrium contain a linear restoring force. Therefore, these systems can be approximated as a simple harmonic oscillator. A damped harmonic oscillator can be described by a second-order differential equation of the following form:

$$m\ddot{x}(t) + c\dot{x}(t) + k_x x(t) = 0 \tag{2.1}$$

where x can be any translational or rotational degree of freedom, m is the mass of the system and k_x its spring constant for this oscillation. Here, $\dot{x}$ is the damping factor with c a constant proportional to the restoring force. This equation can however be written in a more intuitive manner[7], using the damping factor $\gamma = \frac{c}{2m}$ and the resonance frequency $\omega_0 = \sqrt{\frac{k_x}{m}}$:

$$\ddot{x}(t) + 2\gamma\dot{x}(t) + \omega_0^2 x(t) = 0 \tag{2.2}$$

This equation holds for thermally driven oscillations and is solvable. There are three distinguishable cases, depending on the ratio of the damping factor and the resonance frequency: overdamped ($\gamma > \omega_0$), critically damped ($\gamma = \omega_0$) and underdamped ($\gamma < \omega_0$). Most physical systems, such as the experiment described in this thesis, are underdamped, which yields the following solution:

$$x(t) = A \cdot \sin\left(\sqrt{\omega_0^2 - \gamma^2} \cdot t + \phi\right) \cdot e^{-\gamma t} \tag{2.3}$$

where A is the (maximal) amplitude of the oscillation and ϕ its phase. As mentioned in Chapter 1, an important measure for a resonator is its

quality factor. This is a dimensionless value which describes the damping of a resonator. The lower the damping factor is, the higher the Q factor will be. It is defined as the ratio between the frequency of a resonance mode and the energy that is dissipated:

$$Q = \frac{\omega_0}{\Gamma} = \frac{2}{\tau} \tag{2.4}$$

Most of the energy of a system will be stored in the resonance oscillations. Thus, when one measures the spectrum of a resonator, there will be peaks at the resonance frequencies ω_0. The Q factor can be rewritten in terms of the damping time τ:

$$Q = \frac{1}{2}\omega_0\tau \tag{2.5}$$

In an experiment a standard ringdown measurement can be performed on a resonator. Here, the resonator will be driven at its resonance frequency. The amplitude of the oscillation will increase until a maximum is reached, at an equilibrium between the driving and damping forces. At that moment the driving force is turned off and the resonator will only be damped. Its amplitude will thus decrease. From the measured damping time the Q factor can be determined.

Another important measure for quantum mechanical experiments, and in general low amplitude sensing, is the ratio between the temperature and the damping time T/τ. A lower temperature means that there will be less thermal noise over the whole spectrum. The noise spectral density is $S = 4k_BTm\Gamma$, where k_B is the Boltzmann constant and with Γ the frequency is incorporated. It is therefore an advantage to design a mechanical resonator with a given mass m such, to have low resonance frequencies and high Q, in order to have a lower thermal force noise.

The driving of a system can be performed at the resonance frequency. The equation of motion becomes:

$$\ddot{x}(t) + 2\gamma\dot{x}(t) + \omega_0^2 x(t) = F_0 \cdot \cos\left(\sqrt{\omega_d^2 - \gamma^2} \cdot t\right) \tag{2.6}$$

where ω_d is the driving angular frequency and F_0 the fixed amplitude of the driving force. If $\omega_d = \omega_0$ the system will resonate and the amplitude can become large. However, for large driving forces the amplitude of the oscillation can become so large, such that it will deviate from its linear dependency on the restoring force.[5] The system will behave as a Duffing

oscillator and a cubic term has to be introduced to the equation in order to describe the non-linearity of the system:

$$\ddot{x}(t) + 2\gamma\dot{x}(t) + \omega_0^2 x(t) + \delta x^3(t) = F_0 \cdot \cos\left(\sqrt{\omega_d^2 - \gamma^2} \cdot t\right) \tag{2.7}$$

where δ is the Duffing parameter. This equation is however generally hard to solve analytically.

2.2 Magnetic levitation

Most micromechanical resonators are composed of a vibrating membrane, as mentioned in Chapter 1. The main contributions to energy dissipation are clamping losses. In order to avoid this dissipation Vinante et al. have presented a system consisting of a magnetic microparticle levitated in a superconducting well.[6] This experiment has been replicated in order to improve the energy dissipation and obtain higher Q factors.

Our system consists of a spherical microparticle with a radius of 7.9 μm and an assumed saturated magnetisation of 700 mT. The particle is placed at the bottom of a cylindrical shaped hole in a piece of lead, which is a metal that becomes superconducting at a temperature below 7.19 K.[8] Because lead is a type I superconductor it will expel the magnetic field because of the Meissner effect, as will be further discussed in the following section. As a result, a force will act from the superconductor on the particle and, because of the symmetry of the system, the particle will levitate in

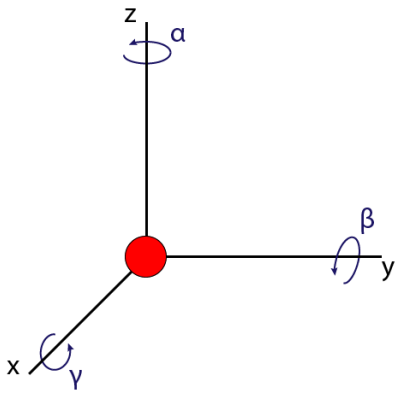

Figure 2.1: *Coordinate system of the experiment with the translational and rotational degrees of freedom.*

the middle of the trap at an equilibrium between the Meissner effect and gravity.

For the well a type I superconductor is chosen because a type II superconductor will obtain magnetic vortices. The magnetic field from the particle would partially go through the material, creating a lattice of normal metal in between the superconducting metal. This would result in a much smaller counter force on the particle, if there at all, and the particle would be pinned at the center at the bottom of the well.

Figure 2.1 shows the three rotational directions of the particle with respect to the coordinate system.

2.3 Meissner effect

Superconductors have two key electrodynamic properties: they have zero resistance and they exclude the magnetic field.[9] How a superconductor behaves around electric and magnetic fields is described by the London equation[10]:

$$\begin{aligned} \frac{d\vec{J}}{dt} &= \frac{n_s e^2}{m}\vec{E} \\ \vec{\nabla} \times \vec{J} &= \frac{-n_s e^2}{m}\vec{B} \end{aligned} \tag{2.8}$$

where $\vec{J}$ is the superconducting current, n_s is the number density of superconducting electrons and e and m are the electron's charge and mass. When one applies Ampère's law on the latter London equation one obtains the London penetration depth:

$$\lambda = \sqrt{\frac{m}{\mu_0 n_s e^2}} \tag{2.9}$$

This is the distance to which a magnetic field penetrates a superconducting material and becomes $1/e$ times it's value at the surface. In this region the lead will be normal. The magnetic field inside the lead is thus:

$$H(z) = H(0) \cdot e^{\frac{-z}{\lambda}} \tag{2.10}$$

where H is the field inside the lead. The London penetration depth depends on the temperature and the critical temperature of the material. An empirical relation is:

$$\lambda(T) \approx \lambda(0) \cdot \frac{1}{\sqrt{1-(\frac{T}{T_c})^4}} \tag{2.11}$$

Which in our case for a temperature of 10 mK and where the lead is far thicker than λ, it becomes $\lambda(T) \approx \lambda(0)$. The Meissner effect thus excludes the magnetic field. However, because the lead cylinder has far more mass than the magnetic particle the inverse force will push the particle upwards. It will levitate at an equilibrium between the Meissner effect and gravity.

2.4 Levitated microparticle

2.4.1 Resonance frequency and frequency shift

A consequence of the non-linearity of the system is a shift in resonance frequency, meaning that for large amplitudes the oscillation will have a deviated frequency.[11] Neglecting dissipation for now, we get the Duffing-like equation of motion. When the system is driven at a resonance frequency of a certain mode that only this mode will gain a large amplitude. Therefore, we can neglect higher order terms of the other modes. In the following, properties only for the z and β modes for one sample will be calculated, since these resonance frequencies can be accurately analytically calculated.[6] We make the assumption to have the particle on an infinite plane, which is possibly since the diameter of the particle is much smaller than the width of the well.

The potential energy of the z and β oscillation of the magnetic particle close to a superconductor is:

$$\begin{aligned} U &= -\frac{1}{2}\int_V \vec{M}(\vec{x}) \cdot \vec{B}(\vec{x}) d\vec{x} + mgz \\ &= \frac{\mu_0 \vec{\mu}^2}{64\pi z^3} \cdot (1+\sin^2(\beta)) + mgz \end{aligned} \tag{2.12}$$

where $\vec{M}, m$ and V are respectively the magnetisation, the mass and the volume of the particle. μ_0 is the vacuum permeability. The magnetic moment is given by $\vec{\mu} = \frac{B_r V}{\mu_0}$. The equilibrium angle of the particle can be found by minimising the potential energy, which results in $\beta_0 = 0$. Thus, the particle is positioned with its magnetic moment horizontal, as shown in Figure 2.2. We use this result to minimise U and find the equilibrium height:

$$z_0 = (\frac{3\mu_0|\vec{\mu}|^2}{64\pi mg})^{\frac{1}{4}} \tag{2.13}$$

For our system this gives $z_0 = 113\ \mu$m. The spring constants of the z- and β -oscillation can be found with:

$$k_z = (\frac{d^2U}{dz^2})_{z_0,\beta_0} = \frac{3\mu_0|\vec{\mu}|^2}{16\pi z_0^5} \tag{2.14}$$

$$k_\beta = (\frac{d^2U}{d\beta^2})_{z_0,\beta_0} = \frac{\mu_0|\vec{\mu}|^2}{32\pi z_0^3} \tag{2.15}$$

This gives $k_z = 5.38 \cdot 10^{-6}\ \frac{N}{m}$ and $k_\beta = 1.15 \cdot 10^{-14}\ \frac{N}{m}$. Now we can find the angular frequencies, considering that the moment of inertial of a perfect sphere is $I = \frac{2}{5}\ mR^2$:

$$\omega_z = \sqrt{\frac{k_z}{m}} = \sqrt{\frac{4g}{z_0}} \tag{2.16}$$

$$\omega_\beta = \sqrt{\frac{k_\beta}{I}} = \sqrt{\frac{5z_0g}{zR^2}} \tag{2.17}$$

This gives $\omega_z = 589\ \frac{rad}{s}$, or $f_z = 93.8$ Hz, and $\omega_\beta = 5441\ \frac{rad}{s}$, or $f_{beta} = 866$ Hz.

When the resonator obtains a large amplitude the following frequencies are expected:

$$\tilde{\omega}_z = \omega_z(1 - \frac{35}{48}\frac{A_z^2}{z_0^2}) = \omega_z - d\omega_z \tag{2.18}$$

$$\tilde{\omega}_\beta = \omega_\beta(1 - \frac{1}{4}A_\beta^2) = \omega_\beta - d\omega_\beta \tag{2.19}$$

where A_z and A_β are the amplitudes of the z and β modes respectively. $d\omega_z$ and $d\omega_\beta$ are the frequency shifts. This can be rewritten in a more insightful way:

$$A_z = \pm z_0 \cdot \sqrt{\frac{48}{35}\frac{d\omega_z}{\omega_z}} \tag{2.20}$$

$$A_\beta = \pm 2\sqrt{\frac{d\omega_\beta}{\omega_\beta}} \tag{2.21}$$

2.4.2 Magnetic field produced by particle and coupling

In this subsection the coupling will be calculated for the most favourable conditions. For example, the magnetisation of the particle is taken to be in the vertical direction, perpendicular to the surface of the pick up coil. In Chapter 4 this will be compared with the expected coupling for the geometry of the experiment.

The movement of the magnetic particle causes a changing magnetic field and will induce a current in the pick up coil, which, in turn, will be detected by the SQUID. This will be further discussed in Chapter 3. There can thus a coupling be found between the particle's position and the measured signal[5, 12]. We start with the magnetic field produced by a magnetic dipole[13]:

$$\vec{B}(z,\theta) = \frac{\mu_0|\vec{\mu}|}{4\pi z^3} \cdot (2\cos(\theta)\hat{\vec{r}} + \sin(\theta)\hat{\vec{\theta}}) \tag{2.22}$$

where z is the distance from the particle to the pick up coil along the z-axis and θ is the angle from this axis, as shown in Figure 2.2. The particle is levitating above a superconductor. Due to the Meissner effect the magnetic field will have a certain penetration depth in which the lead will be normal. This system can be modeled as a dipole at distance z_0 above the surface and an image dipole at the same distance below the surface. Because of the cylindrical symmetry of the system all flux through the coil x- and y-direction will cancel out. We can thus take just the first term of Equation 2.22 and find a total magnetic field of:

$$\begin{aligned} B_{total}(z) &= B_{particle}(\theta_{particle}) + B_{image}(\theta_{image}) \\ &= \frac{\mu_0|\vec{\mu}|}{2\pi} \cdot \left[\frac{1}{(h+d-z_0)^3} \cdot \cos(\theta_{particle}) + \frac{1}{(h+d+z_0)^3} \cdot \cos(\theta_{image}) \right] \end{aligned} \tag{2.23}$$

where the distances to the dipole and image dipole $(h + d \pm z_0)$ are used, where h is the height of the trap and d the distance between the trap and the pick up coil. The flux through the coil is found by an integral over its surface:

$$\Phi = \int\int B_{tot} dA \tag{2.24}$$

where $dA = dxdy = r \cdot drd\phi \approx (h + d \pm z_0)^2 \cdot \tan(\theta) \cdot d\theta d\phi$, where a series expansion for small θ is used. The change in flux caused by the movement of the particle is given by:

$$\Delta\Phi = \int\int (\frac{d}{dz}B_{tot})_{A_z} dA \tag{2.25}$$

where the derivative is taken for the particle moving from equilibrium to its maximal amplitude. This gives:

$$\begin{aligned}\Delta\Phi = \frac{3\mu_0|\vec{\mu}|}{2\pi} \cdot \Bigg| \Bigg\{ & \frac{1}{(h+d-z_0-A_z)^2} \cdot \int_0^{2\pi} \int_0^{\arctan\left(\frac{r}{h+d-z_0-A_z}\right)} \sin(\theta) d\theta d\phi \\ & - \frac{1}{(h+d-z_0)^2} \cdot \int_0^{2\pi} \int_0^{\arctan\left(\frac{r}{h+d-z_0}\right)} \sin(\theta) d\theta d\phi \Bigg\} \\ - \Bigg\{ & \frac{1}{(h+d+z_0+A_z)^2} \int_0^{2\pi} \int_0^{\arctan\left(\frac{r}{h+d+z_0+A_z}\right)} \sin(\theta) d\theta d\phi \\ & - \frac{1}{(h+d+z_0)^2} \int_0^{2\pi} \int_0^{\arctan\left(\frac{r}{h+d+z_0}\right)} \sin(\theta) d\theta d\phi \Bigg\} \Bigg| \end{aligned} \tag{2.26}$$

where r is the radius of the pick up coil. For our experiment this gives $\Delta\Phi = 1.379 \cdot 10^{-10}$ Wb. Now, the current is found by:

$$I(z) = \frac{\Delta\Phi_z}{L} \tag{2.27}$$

The pick up coil has an induction of $L = 156.6$ nH, resulting in a current $I = 880.8\,\mu$A. The energy in the current in the pick-up coil is:

$$U_{coil}(z) = \frac{1}{2} L_{total} I_{coil}^2 \tag{2.28}$$

giving $U_{coil} = 6.074 \cdot 10^{-14}$ J. The total potential energy of the particle in the z mode is:

$$U_{particle}(A_z, \beta_0) = \frac{\mu_0|\vec{\mu}|^2}{64\pi A_z^3} \cdot (1 + \sin^2(\beta_0)) + mgA_z \tag{2.29}$$

This gives an energy of $U_{particle} = 3.984 \cdot 10^{-11}$ J. Note that this is the total potential energy of the particle, where the amplitude that is found in Chapter 4 has been used, and not the energy of the oscillation, which is given by:

$$U_z = \frac{1}{2} k_z z^2 = \frac{1}{2} m\omega_z^2 z^2 = 1.93 \cdot 10^{-25}\, J \tag{2.30}$$

The coupling is defined as:

$$\beta_z^2 = \frac{U_{coil}(z)}{U_z(z)} \tag{2.31}$$

This gives a coupling for an optimal geometry of $\beta_z^2 = 1.525 \cdot 10^{-3}$.

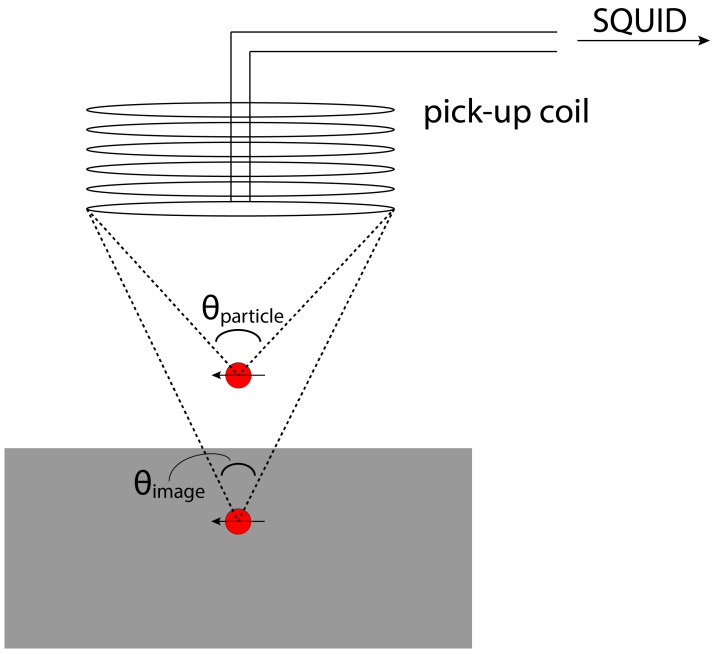

Figure 2.2: *Scheme of the bottom of the trap with the particle at height z_0 and an image dipole at a distance z_0 from the surface of the lead. The particle and image make each make a specific angle θ with the pick up coil.*

2.5 Damping factors

There are several mechanisms that cause dissipation of energy from the resonator. The first is viscous damping. This is caused by the particle moving through the remaining gas in the chamber. Naturally, the higher the pressure, the higher the damping is. There are however also other properties, such as the chemical composition of the gas. Viscous damping was the leading dissipation in Vinante's experiment. Their experiment is performed at 4 K, which yielded a pressure of $P = 10^{-4}$ mbar. The ideal gas law states that a decrease in temperature brings a decrease in

pressure. Therefore, since our system can be cooled down to 10 mK, which is two order of magnitude less, we will have a pressure below 10^{-9} mbar to perform our experiment at. We thus expect to have less viscous damping and have a higher Q factor.

2.5.1 Viscous damping

z mode

In this subsection we will discuss the z oscillation. For a sphere around 90% of viscous damping comes from drag and around 10% from skin friction, which we will therefore neglect. For small velocities, as we will have in our experiment, the force that the gas acts on the particle is linear with the particle's velocity:

$$F_{drag} = \frac{1}{2}\rho v C_D A \tag{2.32}$$

where $C_D = 0.47$ is the drag coefficient for a sphere and $A = 2\pi R^2$ the cross sectional area of the particle. The density of the gas is given by:

$$\rho = \frac{MP}{R_{gas}T} \tag{2.33}$$

with M the molar mass of the gas (which at these temperatures can be assumed to be pure helium), P the pressure, R_{gas} the universal gas constant and T the temperature. Filling this in with $P = 10^{-9}$ mbar and $T = 30$ mK gives a density and force of:

$$\rho = 1.605 \cdot 10^{-14}\ \frac{kg}{m^3} \tag{2.34}$$

$$F_{drag} = 4.893 \cdot 10^{-35}\ N \tag{2.35}$$

With this we can find the dissipation rate:

$$\Gamma_{z,drag} = F_{drag} \cdot v = 4.687 \cdot 10^{-43}\ \frac{J}{s} \tag{2.36}$$

With the total energy of the oscillation, given by Equation 2.30, the Q factor can be found:

$$Q_{z,drag} = \omega_z \cdot \frac{U_z}{\Gamma_{z,drag}} = 1.83 \cdot 10^{12} \tag{2.37}$$

β mode

We can now do the same for the β oscillation. However, since here the particle is not displaced but only rotated, we can assume to have viscous damping 100% coming from skin friction. To find the energy dissipation we now need the torque instead of the force on the particle:

$$\tau = -8\pi R^3 \eta \omega_\beta \tag{2.38}$$

where the viscosity is given by:

$$\eta = \rho\lambda \cdot \sqrt{\frac{2k_\beta T}{\pi M}} \tag{2.39}$$

The mean free path λ of the helium atoms is:

$$\lambda = \frac{k_B T}{\sqrt{2}AP} = 1.04 \cdot 10^{-4}\, m \tag{2.40}$$

At the same parameters as for the z-oscillation this gives a viscosity and torque of:

$$\eta = 1.35 \cdot 10^{-29}\, Pa \cdot s \tag{2.41}$$

$$\tau = 4.18 \cdot 10^{-39}\, Nm \tag{2.42}$$

This results in a dissipation rate of:

$$\Gamma_{\beta,drag} = \tau \cdot \omega_\beta = 1.53 \cdot 10^{-35}\, \frac{J}{s} \tag{2.43}$$

The total energy of the β mode, assuming an amplitude of 45°, is given by:

$$U_\beta = \frac{1}{2}\kappa\theta^2 = 1.39 \cdot 10^{-25}\, J \tag{2.44}$$

Which leads to a Q factor of:

$$Q_{\beta,drag} = \omega_\beta \cdot \frac{U_\beta}{\Gamma_{\beta,drag}} = 4.95 \cdot 10^{13} \tag{2.45}$$

2.5.2 Eddy currents

z mode

Another mechanism that causes energy dissipation is eddy currents. When a changing magnetic field is near a normal conductor it induces loops of electrical current within the conductor. This is due to Faraday's law. Although in our experiment the particle is completely confined by a superconductor and an insulator, eddy currents can still occur. This comes from the Meissner effect, which states that there is a certain penetration depth in the superconductor for the magnetic field. As a consequence the material within this region will be a normal conductor. This is where eddy currents will occur. These currents feel an effective resistance, which cost energy, and are therefore damping the motion of the particle.

Eddy currents depend on the specific geometry, which in our case makes it harder to calculate analytically. However, we can estimate the losses by assuming a spherical geometry. The dissipation rate is given by:

$$\Gamma_{z,eddy} = \frac{\pi}{15} B^2 R^2 \omega_z^2 \sigma \tag{2.46}$$

where $\sigma = 4.55 \cdot 10^6 \, \frac{S}{m}$ is the electrical conductivity of the lead and B the change in magnetic field. This gives:

$$\Gamma_{z,eddy} = 8.07 \cdot 10^{-34} \, \frac{J}{s} \tag{2.47}$$

$$Q_{z,eddy} = \omega_z \cdot \frac{U_z}{\Gamma_{z,eddy}} = 1.11 \cdot 10^{11} \tag{2.48}$$

β mode

For the β oscillation the equation is slightly altered as follows:

$$\Gamma_{\beta,eddy} = \frac{\pi}{15} B^2 R^5 \omega_{beta}^2 \sigma = 1.52 \cdot 10^{-42} \, \frac{J}{s} \tag{2.49}$$

This gives:

$$Q_{\beta,eddy} = 4.95 \cdot 10^{20} \tag{2.50}$$

2.5.3 Joule heating

Besides this, a far larger dissipation factor would be to have a resistance in the otherwise superconducting pick up coil- or SQUID-circuit. The current through the circuit would generate heat, which costs energy. In Chapter 4 will be shown how this is problematic for this experiment. The power dissipated is quadratic with the current through the circuit:

$$\Gamma_{res} = I^2 R \tag{2.51}$$

As calculated above, the current generated for the z mode is $I_z = 880.8\mu$A.

Chapter 3

Methodology

3.1 Dilution refrigerator

In order to do quantum mechanical measurements the internal energy of the system needs to be reduced to near the ground state of the system. This is done by cooling the system down to mK temperatures with a dry dilution refrigerator (Leiden Cryogenics), which is shown in Figure 3.1. The process of cooling down goes as follows: first, gaseous helium is pumped through the system, after which it goes through the pulse tube. This alternately compresses and decompresses the helium, which is an exothermic process, such that each cycle energy is extracted from the system. With this process the 4K plate can reach a temperature of 3.4 K. Now, ^4He is cycled through a closed system that goes through the mixing chamber and the still. This is cooled down and at some point liquid ^4He will stand in the mixing chamber and still, see Figure 3.1. Now, ^3He is pumped into the system. The key property used in the mixing process is that ^4He are bosons and ^3He are fermions.[14] This means that all ^4He atoms can occupy their lowest energy state. The ^3He will mix with the ^4He inside the mixing chamber and still. By doing this, the entropy of the system increases, which, by the third law of thermodynamics, will remove energy from the system. A liquid mixture of the two will now stand in the mixing chamber and the still. An equilibrium will be attained of 6% liquid ^3He and 94% ^4He. At the surface however ^3He evaporates and is circulated back through the system. With this continuous process the system can reach its ground temperature of 10 mK.

Our experiments were mounted on the mixing chamber plate.

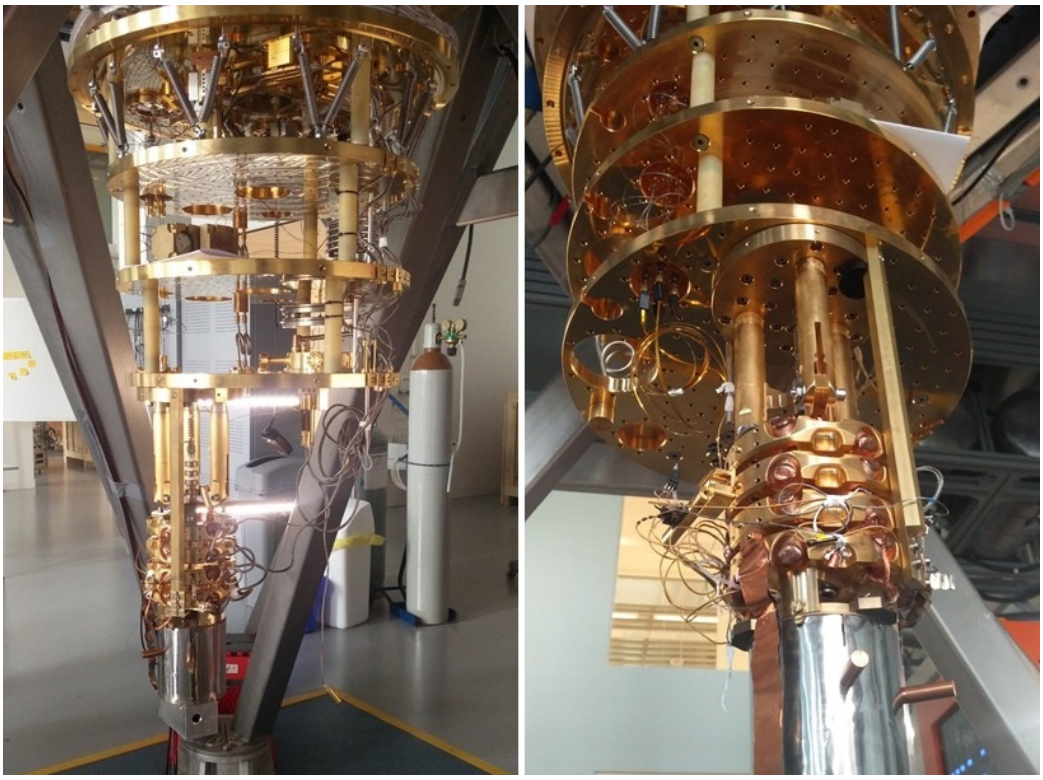

Figure 3.1: *Left: photograph of the dilution refrigerator. The mixing chamber is located at the bottom plate. Note that the still plate is attached with springs to prevent vibrations being transmitted to the mass spring system. Right: Photograph of the mass spring system, a low pass vibration isolation system.*

3.2 Vibration isolation and thermal conductance

As will be discussed in the next Section, the signal coming from the levitating particle is detected with a SQUID. If the particle is oscillating with a certain frequency, a current with the same frequency is generated. However, there will always be multiple sources of vibrations in the system, also causing currents through the SQUID. The challenge is to find which part of the signal is caused by the experiment. Also, these vibrations raise the noise floor, but could also prevent the experiment from cooling down, both of which would make this experiment impossible. For these sensitive measurements it is therefore necessary to have vibration isolation in the system.

The first solutions are to place the pumps in a separate room and mounting the cryostat on a heavy platform. The pulse tube however will create vi-

brations inside the cryostat. There will also be external vibrations that are not damped. This creates a challenge to decouple the sample from these vibrations while maintaining a functional heat conductance. As shown in Figure 3.1, every plate is connected to the plate above via links. The vibration isolation is better for a lower stiffness of these links, while the thermal conduction depends on the cross-sectional area of the thermal links. The system is optimised for both factors.

In this dilution refrigerator there are four vibration isolation systems present. First, the cryostat is installed on a separate platform of 25 tons of concrete, supported on passive hydraulic vibration isolation dampers. The second consists of seven dampers which are installed on the large concrete slap underneath the system. These dampers are also used to induce vibrations with specific frequencies in order to drive the magnetic particle, as will be discussed in Section 3.4. There are two in the x-, two in the y- and three in the z-direction, which acts as low-pass filters.

The third step in isolation is a mass-spring system. The bottom half of the cryostat hangs on springs, which are connected between the 4K plate and the still plate, as shown in Figure 3.1. This is a low-pass filter.

The fourth isolation system is again a mass-spring system, consisting of four masses connected in series.[15] Each level is a second order filter with a corner frequency of 100 Hz, which adds 40 dB per decade of filtering. It is important to note that the damping is caused by reflection, not by dissipation, which is crucial to keep the system at a low temperature. The masses are connected with heat links made of soft braided copper in order to maintain a working heat link while remaining a low stiffness.

These systems together form the sophisticated arrangement which is necessary for quantum mechanical measurements and enables this experiment of the levitated microparticle.

3.3 SQUID detection

Measurements were performed on multiple experiments. However, in the following sections we will focus on one of these samples. The pick up coil above the trap encloses part of the magnetic field coming from the levitating particle. The change of flux enclosed by the coil induces a current, which is transferred to the SQUID. This is done by a two-stage de-

tection system, as this way the inductance of the SQUID is more equally matched with that of the pick up coil.[15, 16] A diagram of the circuit is shown in Figure 3.2. More equal inductances results in a better coupling, and thus a more sensitive device. A SQUID (Magnicon low noise 2stage DC SQUID) with an inductance of $L_{in} = 150$ nH is used. A transformer is placed between the pick up coil ($L_{pickup} = 156.6$ nH) and the SQUID, where the inductance of the primary coil is $L_{f_1} = 0.72$ nH and of the secondary coil $L_{f_2} = 360$ nH. With the mutual inductances of $M_{1,2} = 14.5$ nH and $M_{2,SQUID} = 2.44$ nH the flux that is generated in the SQUID can be calculated:

$$\Phi_{SQUID} = \frac{M_{1,2}M_{2,SQUID}}{L_1 L_2 - M_{1,2}^2} \cdot \Phi_{pickup} \tag{3.1}$$

where $L_1 = L_{pickup} + L_{f_1} + L_{par}$ is the total inductance of the pick up coil circuit and $L_2 = L_{in} + L_{f_2} + L_c$ is the total inductance of the transformer. It is evident that the inductance of the pick up coil can be chosen such, as to have optimal coupling to the SQUID. It is however a challenge to then also have a good coupling to the magnetic particle.

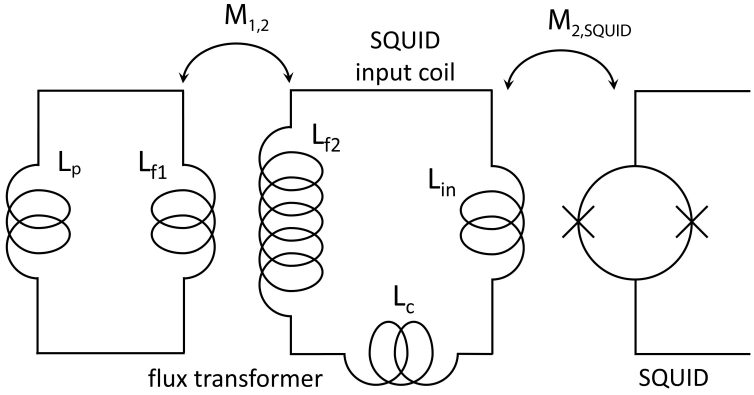

Figure 3.2: *Diagram of the superconducting detection circuit. The magnetic flux coming from the particle in the pick up coil is transferred to the SQUID input coil through a transformer. Adapted from [15].*

If we fill in Equation 3.1 for our experiment, we find $\Phi_{SQUID} = 3.63 \cdot 10^{-4} \cdot \Phi_{pickup}$. Therefore the coupling between the pick up coil and the SQUID is about 0.0363%.

This taken together with the coupling calculated in Chapter 2 gives a total coupling of $5.534 \cdot 10^{-7}$ for the z mode.

3.4 Setup and fabrication

First, it was attempted to replicate the experiment of Vinante et al. with some adjustments in the design. The magnetic microparticle is made of neodymium-iron-boron (NbFeB). A grain of powder with the desired spherical shape and size is chosen under a microscope. Particles with a radius between 7.9 and 15 μm have been used and are magnetised in a 6 T field. As mentioned in Chapter 2, the mass of the particle alters the equilibrium height and the resonance frequencies. The particle is picked up with a needle by electrostatic force. Therefore, larger particles are harder to stick to the needle and be picked up. Then, it is gently placed at the bottom and the middle of the lead trap, as shown in Figure 3.3. The trap is a cylindrical hole in a piece of lead with a diameter of 1.75 mm and depth of 0.75 mm.

Next, the pick up coil and driving loop are placed above the particle. Several designs have been used. A spool was designed with the desired diameter and distance to the particle, such that a relatively high coupling achieved and that it also acted as a lid on the well. This way the particle could not accidentally fall out during transfer of the sample. A diagram and photo of the spool is shown in Figure 3.4. The spool is made of PEEK, a material which can be used in UHV and cryogenic systems. A disadvantage is that, since it is a plastic, it can be electrostatically charged. There is therefore a possibility for the particle to become stuck to the spool. To prevent this from happening an alpha radiator was used to neutralise the

Figure 3.3: *Optical microscopy picture of the inside the lead trap with the magnetic particle is laying at the bottom. This is an elliptical shaped trap, which will be used for future experiments. The traps used in our samples are circular.*

spool. A pick up coil with six windings of 50 μm Nb wire was placed at the top axis and a driving loop of the same wire at the bottom axis.

The well was fixated on a copper plate to assure a good thermal conductance, as shown in Figure 3.5, and the pick up coil was connected to a SQUID in a Nb casing. The whole sample was closed in an Al container. The sample was then installed on the mixing chamber plate of the cryostat, as shown in Figure 3.5.

Our experiments were mounted on the mixing chamber plate.

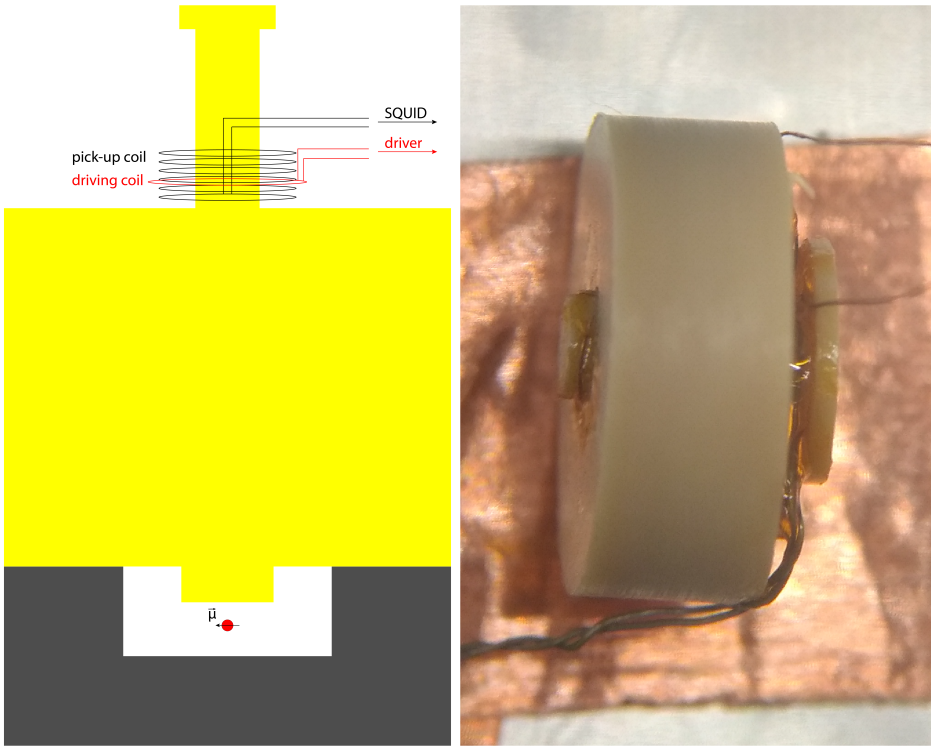

Figure 3.4: *Left: Simplified scheme of the designed spool and trap. The pick up coil and the driving loop are placed at a distance d from the top of the trap. The spool was partly placed inside the trap, such that the particle can move freely. Right: Close-up photograph of a similar spool. Here, the driving loop is placed beneath the spool.*

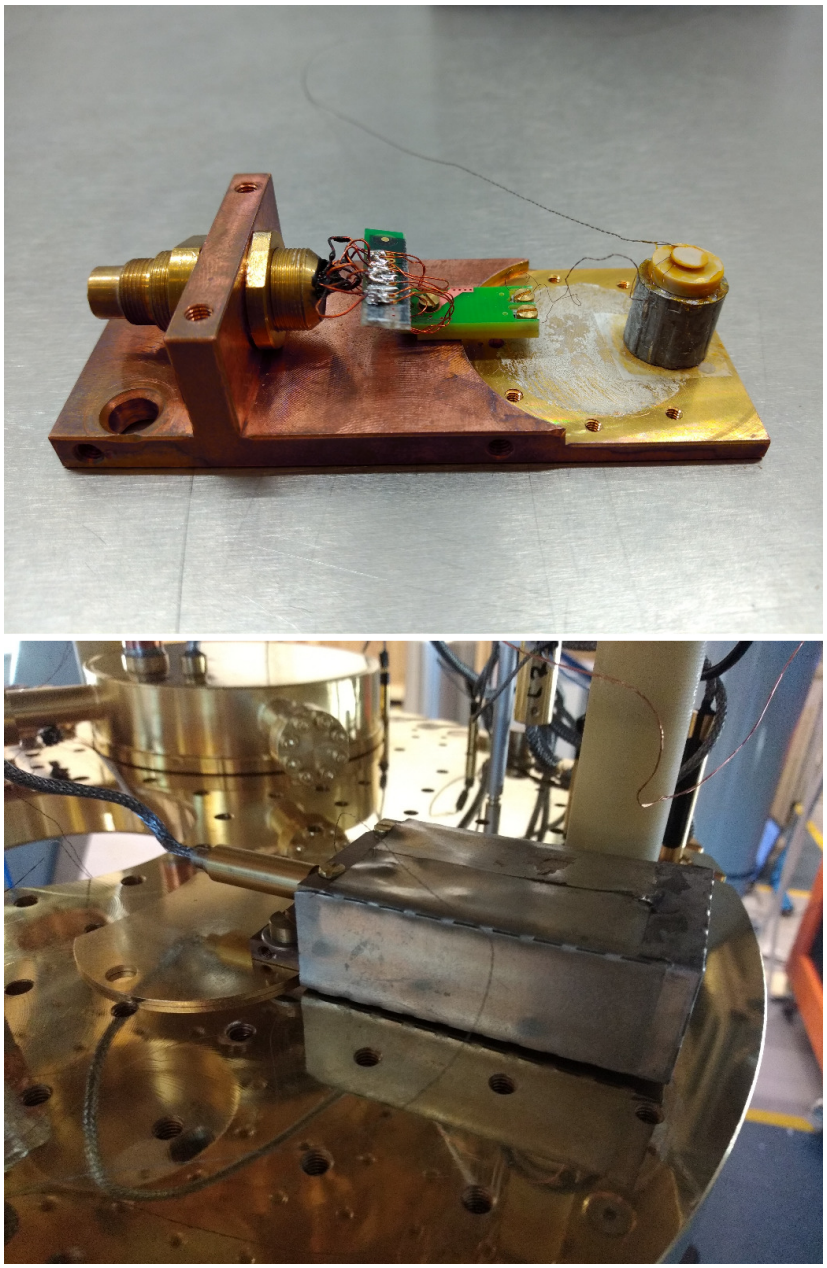

Figure 3.5: *Top: Photograph of the sample without Nb casing. The pick up coil is connected to the SQUID. Bottom: Photograph of the sample installed on the mixing chamber plate.*

3.5 Simulation

Finding the configuration of a magnetic system requires complex calculations of magnetic fields. Often, this is done with a finite element analyses of a three-dimensional space. This, however, requires a lot of computer power and long computational times. Here, the magnetic system of the experiment is simulated using the Magpylib Python package[17], which uses analytical solutions to provide good approximations of the magnetic field.

The particle is simulated by a sphere placed at the origin, with a magnetisation in the x-direction. When the particle moves the flux difference through six loops above the particle is calculated, each inducing a certain current through the loop. The magnetic field strength produced by the particle is shown in Figure 3.6. The geometry and the magnetic field strength inside one loop is shown in Figure 3.7. Since in the experiment the flux is picked up with a coil, these loops are now treated as current sources placed in series, resulting in a total current through the coil. The six rigid body modes z, x, y, β, α and γ have been simulated.

Two geometric simplifications have been used. As mentioned above, the coil is replaced by six individual loops. This will alter the calculated current, because the induction of the coil will be different. This could however be improved by letting the loops interact with each other by the magnetic field that each creates. A second distinction between the experiment and the simulation is the absence of the superconducting trap, which results in two effects. First, magnetic field is not confined by the cylindrical well, resulting in a different flux through the loops. Second, the material in the region of the penetration depth will have a magnetic moment, which is not simulated. However, this simulation provides a good approximation for our experiment.

The energy transferred to the current, as in Equation 2.28, is calculated for all six modes. The coupling, as in Equation 2.31, is calculated for the z and β mode. Besides this, the effect of a misaligned pick up coil is simulated. This is done for the coil tilted in the y-direction by 0° to 3° and the coil displaced by 0 to 0.3 mm in the x-direction.

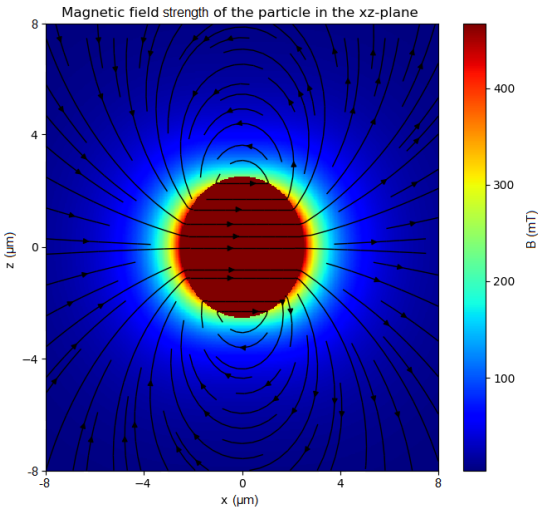

Figure 3.6: *Simulation of the magnetic field stenght of the particle in the xz-plane.*

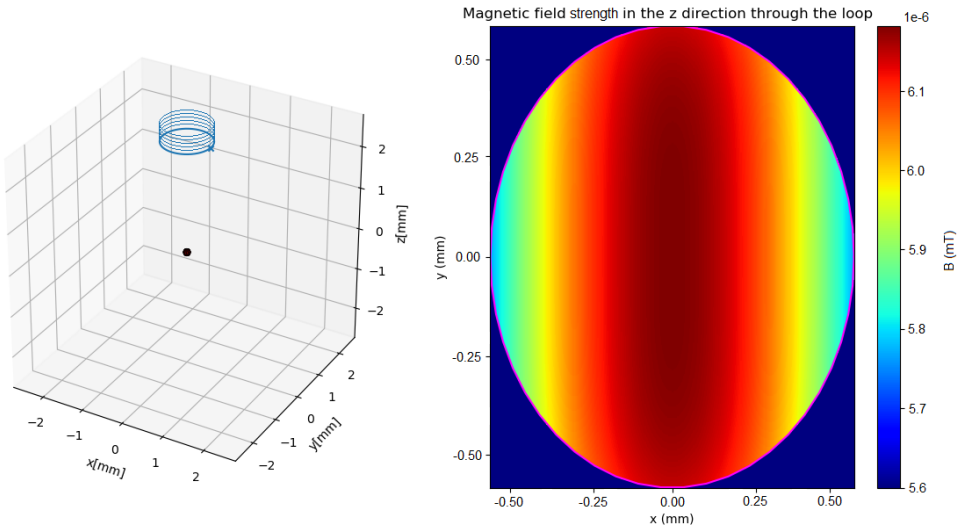

Figure 3.7: *Left: Geometry of the magnetic particle and the pick up loops in the simulation. Note that the particle is 10 times magnified. Right: The magnetic field strength on the surface of the bottom pick up loop.*

Chapter 4

Results & Discussion

4.1 Simulation

A simulation of the system can give insights in the results to expect in the experiment. As described in Chapter 3, the current induced in the pick up coil has been simulated for a single period of oscillation of the magnetic particle. This is done for all six rigid body modes and is shown in Figure 4.1. Since the experiment is simulated for an optimal geometry, there is a perfect cylindrical symmetry. Therefore, an equal current is expected for the x and y modes. Note that the amplitude as found from the ringdown measurements of the z mode has been used for all translational modes. A smaller amplitude of the oscillation would only alter the amplitude of the current. It can, however, be seen that the z mode induces a much higher current than the other translational modes. Which is clear, since there is a larger flux difference during the oscillation due to the horizontal magnetisation of the particle. Figure 4.1 shows that the frequency of the induced current from the x and y modes is twice the frequency of the oscillation of the particle. Due to the symmetry of the system there is also an equal current for the β and γ modes. For the rotational degrees of freedom an amplitude of 45° has been used. However, a lower amplitude would result in a smaller current. This also explains why the current from the β and γ modes shows a jump between the left and right hand side of the graph when the oscillation is at the maximum amplitude. These modes could be distinguished from each other by breaking the symmetry of the system, for example by using an elliptically shaped trap or aligning the pick up coil not perfectly above the middle of the trap.

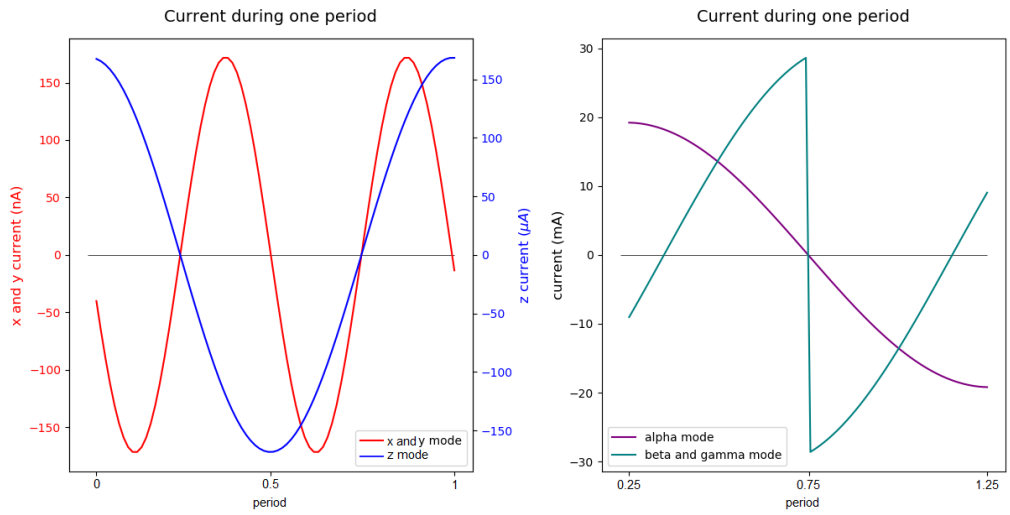

Figure 4.1: *Simulated current induced by the translational and rotational modes of the particle.*

The energy of the induced current is simulated for all modes and is shown in Table 4.1. The effect of a tilted pick up coil is shown in Figure 4.2 and 4.3. Different scales have been used since there are large differences in energy. As expected, the energy of the z mode increases for a greater angle, since more magnetic flux is picked up by the coil. For an angle of $0°$ the energy of the x and y mode are equal. An opposite behaviour of the x and y mode, and of the β and γ mode, is expected, as the tilt is in the x-direction. It is therefore breaking these symmetries of the system. It is notable that a nonlinear behaviour is seen for the y and β mode, which is caused by the dipole field of the particle.

Table 4.1: *The energy of the induced current for all oscillations.*

mode	energy (J)
x	$2.22 \cdot 10^{-15}$
y	$2.22 \cdot 10^{-15}$
z	$2.32 \cdot 10^{-21}$
α	$2.89 \cdot 10^{-11}$
β	$6.41 \cdot 10^{-11}$
γ	$6.41 \cdot 10^{-11}$

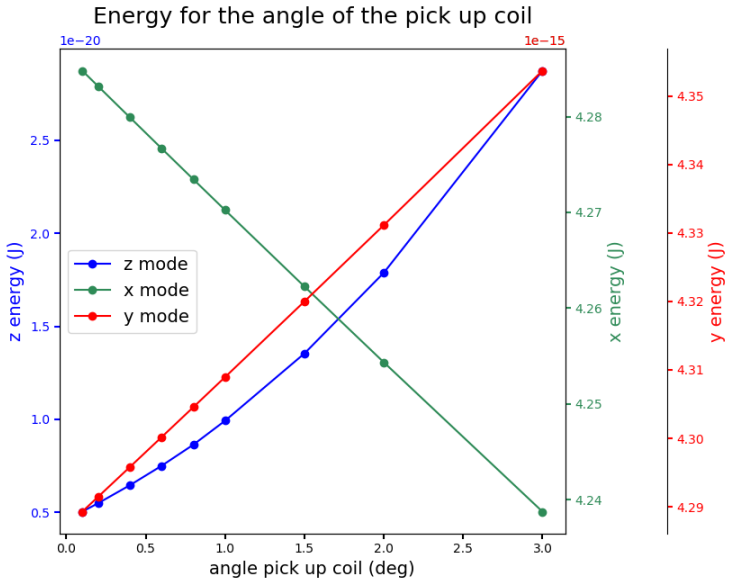

Figure 4.2: *Simulated energy of the induced current of the translational modes of the particle for different angles of the pick up coil.*

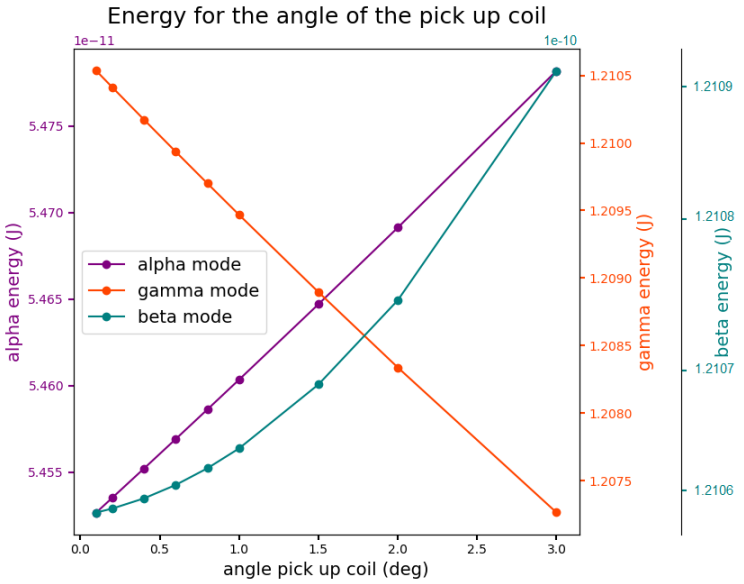

Figure 4.3: *Simulated energy of the induced current of the rotational modes of the particle for different angles of the pick up coil.*

The effect on the energy of the induced current of a misalignment in the x direction of the pick up coil is shown in Figures 4.4 and 4.5. Again, for a misalignment of $0mm$ the energy of the x and y mode are equal. Here too, an opposite behaviour of the x and y mode, and of the β and γ mode, is expected, as the misalignment in the x-direction breaks these symmetries of the system. As expected, the energy of the z mode increases for a greater misalignment, since a larger flux difference is detected by the pick up coil. The energy of the γ mode shows, as expected, an increase, since there is a greater flux difference.

Finally, using Equation 2.31, the coupling of the z and β modes have been calculated. Note that here a geometry comparable to the experiment has been used. It is shown in Figure 4.6. It can be seen that the coupling for both modes increase for a tilted pick up coil. This is expected since a higher current is induced, as discussed above. For the misalignment the coupling of the modes show opposite behaviour. The coupling of the β mode decreases when the coil is shifted in the x-direction. It can therefore be assumed that the coupling for the γ mode would increase. If the shift would be in the y-direction these behaviours would be opposite. Remarkably, the coupling of the z mode has increased four order of magnitude for a shift of 0.30 mm of the pick up coil. It would therefore be beneficial to use this in the design of future samples.

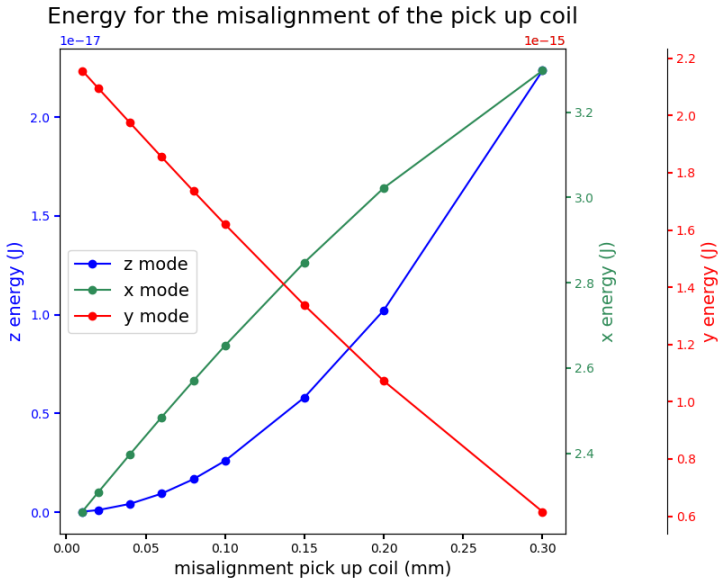

Figure 4.4: *Simulated energy of the induced current of the translational modes of the particle, plotted against the misalignment of the pick up coil in the x direction.*

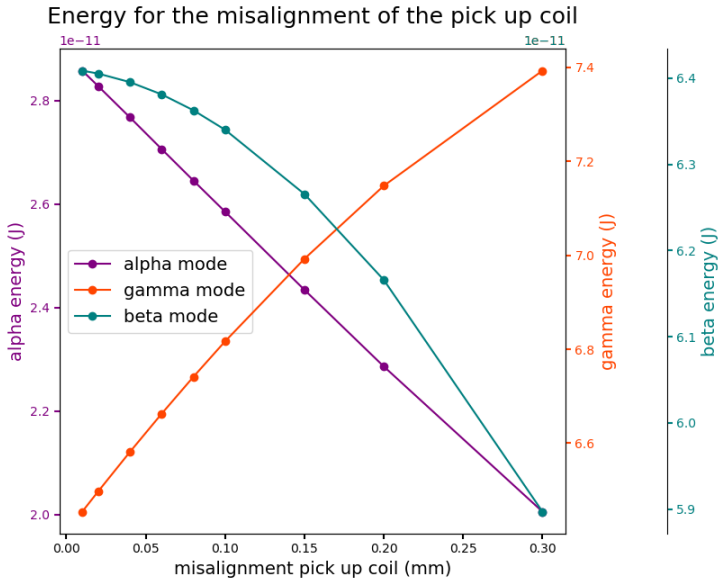

Figure 4.5: *Simulated energy of the induced current of the rotational modes of the particle, plotted against the misalignment of the pick up coil in the x direction.*

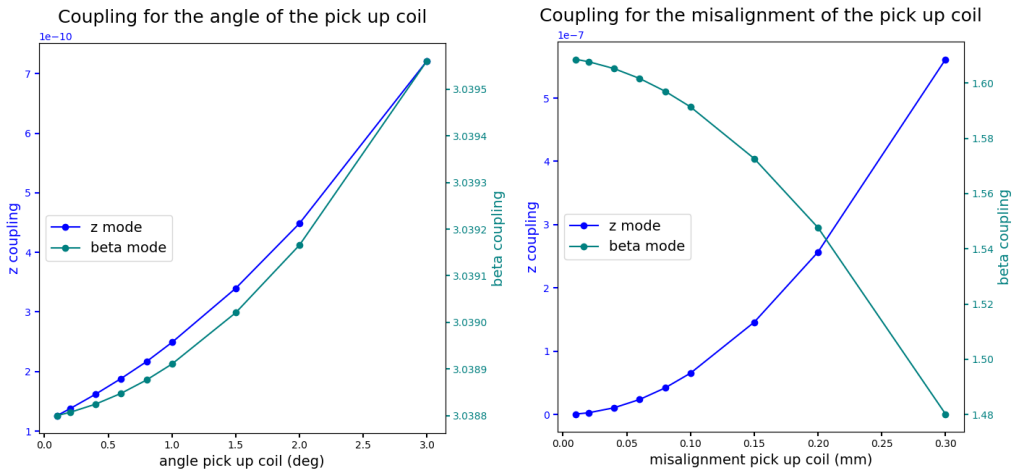

Figure 4.6: *Simulated coupling of the z and β modes of the particle. Left: Plotted against the tilt of the pick up coil. Right: Plotted against the misalignment of the pick up coil in the x direction.*

4.2 Experiments

4.2.1 Large energy dissipation

The first experiments that were performed presented a spectrum as shown in Figure 4.7. It is evident that the power spectral density of the signal decreased rapidly, after the cut-off frequency of ± 100 Hz. This is the behaviour of an RL low-pass filter and thus suggests a resistance present in the superconducting circuit. As a resistance causes energy dissipation through Joule heating, a sample with any resistance will have an extremely low Q factor. The resistance can be calculated from the cut-off frequency f_c:

$$R = 2\pi f_c L \tag{4.1}$$

This results in a resistance of $R \approx 1.4\, m\Omega$. It can be caused by fabrication errors, such as bad contact points. It was thus crucial to solve this and the following samples were fabricated with certain precautions, such as removing unnecessary clamping points, chemical etching the Nb wires with formic acid and sanding of the wires and contact pads.

Assuming that mode is the z oscillation, the dissipation rate from Equation 2.51 is gives $\Gamma_{z,res} = 1.09 \cdot 10^{-9} \frac{J}{s}$. Which results in a quality factor of:

$$Q_{z,res} = \omega_z \cdot \frac{U_z}{\Gamma_{z,res}} = 2.43 \cdot 10^{-14} \tag{4.2}$$

which explains why no resonance peaks were seen.

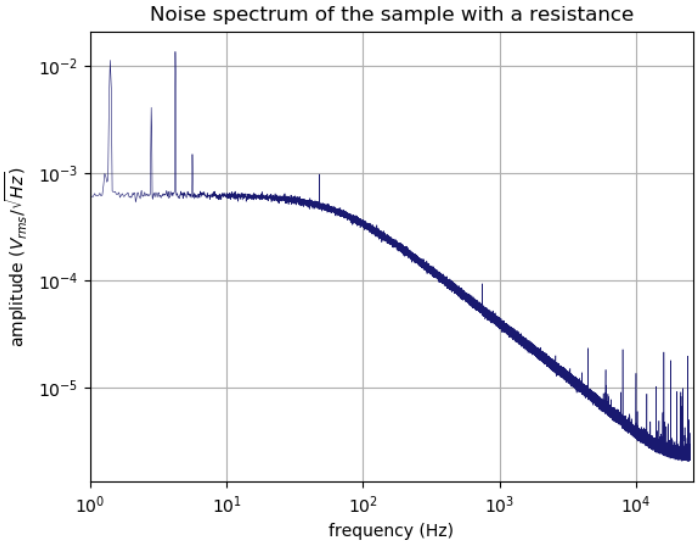

Figure 4.7: *Measured spectrum of the resonator. The kink of decreasing signal is caused by a resistance in the superconducting detection circuit.*

4.2.2 Ringdown measurements

As mentioned in Chapter 3, for the following experiment three samples were installed, two on the mixing chamber plate and one below the mass spring system. Of the last sample the SQUID did not become superconducting, assumably due to a bad heat conduction connection, which made measurements impossible. Also, because of its lower transition temperature, it can be assumed that the lead trap did not become superconducting. This means that the particle would remain pinned down at the bottom of the trap.

The other two samples however were successfully cooled down and measurements could be performed. As before, we will focus on one of these samples, as this gave the most insightful results. Now, a regular spectrum

was obtained without a residual resistance problem. A resonance peak was found at a frequency of 147.786 Hz. The system was mechanically driven at this frequency and a response, noted by an increase of amplitude, was observed. After driving the system for one minute the driving was turned off in order to see a ringdown. A ringdown at this frequency was consistently observed and the ringdown time was significantly larger than that of mechanical modes of the cryostat itself, which can be expected to be below 5 s. Figure 4.8 shows an average of eleven ringdowns and an exponential fit of the data. The normalised residual of the fit is shown in Figure 4.9. It was found that the amplitude was $A = 6.873$ mV and the ringdown time $\tau = 47.48$ s. If we assume this resonance to be the z mode, this results in a quality factor of $Q = 22046$.

This Q factor is much than was expected from the calculations in Chapter 2. One possible explanation is that when the lead undergoes the transition into its superconducting state, magnetic flux could become trapped inside the lead trap. This would come from the Earth's magnetic field, which was not sufficiently shielded. At this point, the magnetic field lines are pinned down and the levitating particle will have to move through these, which costs energy. Thus, the damping factor would be large, resulting in a short ringdown time and a low Q factor.

Another reason could be that the lead is contaminated. This can create regions inside the lead that become superconducting only at temperatures below 10 mK. Therefore, more material from the well would be in its normal state, which causes a weaker Meissner effect and more dissipation due to eddy currents.

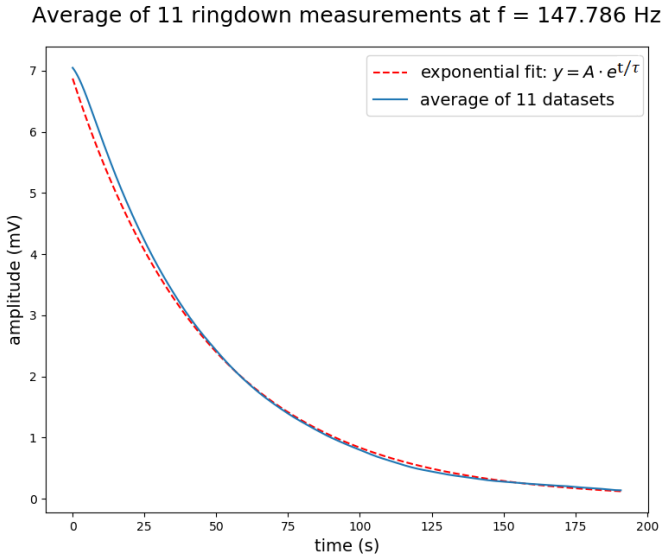

Figure 4.8: *Ringdown measurement at a frequency of* 147.786 *Hz. Data and an exponential fit of the average of eleven measurements.*

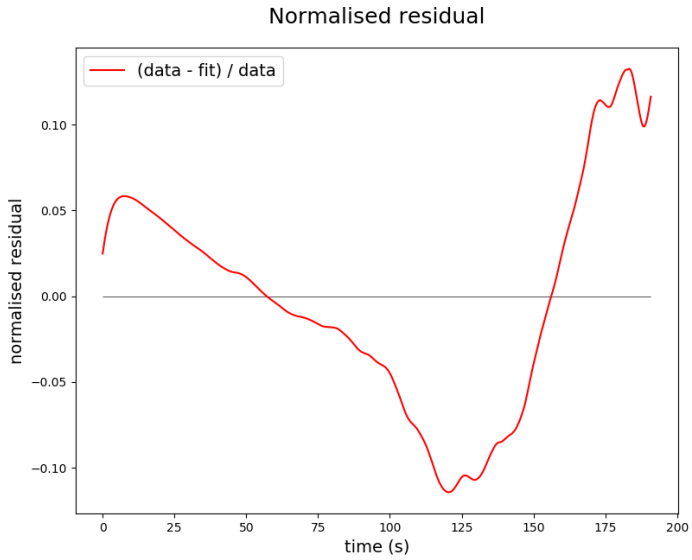

Figure 4.9: *Normalised residual of the exponential fit of Figure 4.8.*

4.2.3 Frequency shift

Vinante et al. observed nonlinear behaviour of the system where the resonance frequency shifted down for higher amplitudes.[6] This shift has been derived for the z and β modes in Chapter 2. Figure 4.10 shows the observed frequency shift during the ringdown measurements at a frequency of $f_0 = 147.786$ Hz. The black graph shows the average of eleven ringdown measurements. As the resonance frequency alters, the signal and the internal clock of the lock-in amplifier will steadily become out of phase. The data from Figure 4.10 is taken from the slope of the phase during the ringdown. At low amplitudes we see that the signal is below the noise floor. As the amplitude goes up the frequency shifts down quadratically, as expected from Equation 2.18 and 2.19. The significant increase at high amplitudes, at the right hand side of the dashed line, is however an artefact. Due to the lock-in time constant used in the experiment the signal from the driving period is still taken along during the first seconds of the ringdown.

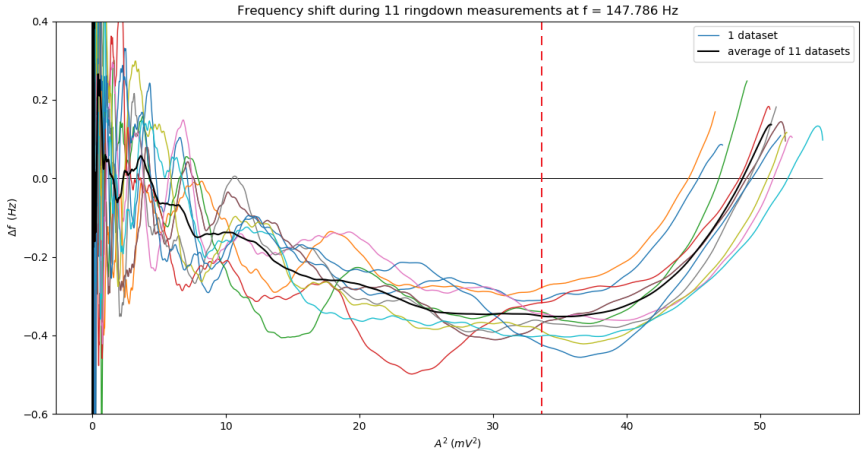

Figure 4.10: *Frequency shift of the resonance mode at a base frequency of* 147.786 *Hz. The black graph is the average of eleven ringdown measurements.*

Assuming this to be the z mode, when we measure a Voltage amplitude of 4.47 mV at a base frequency of $f = 147.786$ Hz we see a frequency shift $d\omega_z = -0.296$ Hz. As calculated before, the equilibrium height is $z_0 = 113\,\mu$m. If we fill this in we find the amplitude of the oscillation:

$$A_z = \pm 5.92\,\mu m \tag{4.3}$$

With this, we can calculate the coupling of this mode, which can be compared with the optimal coupling found in Chapter 2 and simulated coupling in Section 4.1. Equation 2.30 gives:

$$U_z = 2.34 \cdot 10^{-16}\ J \tag{4.4}$$

With a transfer coefficient between the flux in the SQUID and the measured signal of $0.43\ V/\Phi_0$, the energy of the induced current can be found with Equations 2.27 and 2.28:

$$U_{coil} = 4.29 \cdot 10^{-27}\ J \tag{4.5}$$

This results in a coupling of:

$$\beta_z^2 = 1.83 \cdot 10^{-11} \tag{4.6}$$

Note that this is eight orders of magnitude lower than the coupling for the most favourable conditions, as calculated in Chapter 2. This can be explained, since in the experiment the magnetisation of the particle is parallel with the pick up coil, resulting in much smaller magnetic field differences during the oscillation.

The coupling found here is, however, only a factor three lower than the one simulated. This could mean that either the experiment was fabricated extremely symmetric (less than 0.1° oblique and $10\ \mu m$ placed out of the middle of the trap), which seems unlikely. Or the simulation should be improved by more accurately calculating the induced current and by adding the superconducting trap.

Chapter 5

Conclusion & Outlook

To research quantum mechanical effects a sensitive measurement system needs to be developed. For this, the best candidate is a micromechanical resonator that is isolated from its surroundings and thus has an extremely high Q factor. The boundary between quantum and classical mechanics could be investigated by increasing the mass of a system that is brought to its ground state. Here, the first steps have been taken to fabricate and test such a resonator. Also, the experiment has been simulated, where the energy of the current induced by all translational and rotational modes has been calculated. Besides this, the coupling between the z and β mode and the induced current has been calculated. In the experiment, a magnetic microparticle inside a cylindrical lead trap has been cooled down to a temperature of 10 mK. Due to the Meissner effect the particle is levitated, where its movement was measured with the use of SQUID detection.

In the process several challenges were encountered. First, a resistance in the superconducting circuit was detected. This caused so much energy dissipation that a high Q factor could never be obtained. Several trials were performed until a sample fabrication method was developed where no resistance was present.

Another challenge was to have a good coupling between the particle and the SQUID. Finally, a trap and spool have been designed to optimise this coupling and two experiments were cooled down and functional. However, the coupling between the driving loop and the particle was not sufficient. This could be caused by the pick up coil, which screens the particle from the magnetic field produced by the loop. This can be resolved by redesigning the superconducting circuit such, that the pick up coil is also

used as the driver. Ringdown measurements could be performed by consecutively driving the resonator and measuring the induced current with this coil.

The particle could however also be driven by mechanical actuators. The coupling of the z mode has been measured, which differed a factor three with the coupling that was simulated. Ringdown measurements were performed and a resonance was found at a frequency of 147.786 Hz, which could be assumed to be the z mode. The ringdown time was $\tau = 47.48$ s, resulting in a quality factor of $Q = 22046$. This is much smaller than the Q factor expected from theory, which could be explained by flux lines of the Earth's magnetic field becoming trapped inside the lead trap during the superconducting transition. Also, the lead could be contaminated, resulting in a lower critical temperature. Both causes would lead to a large energy dissipation.

The former challenge can be overcome by wrapping the trap in mu-metal. This is a material with a very high magnetic permeability. This would redirect the magnetic field through the mu-metal, instead of through the trap. When the experiment is cooled down there will thus be almost no magnetic field that could be trapped inside the trap. The latter can easily be resolved by using a trap of high purity aluminium, which is a superconductor with a critical temperature of 1.2 K.

With these challenges worked out there will be no source of large energy dissipation present. Then, eddy current losses are expected to become the leading term of dissipation, giving rise to the earlier calculated Q factor of the order of 10^{11}. This opens the road to research quantum mechanical effects and investigate the boundary of quantum and classical mechanics. Also, gravitational measurements can be performed by using the gravity between a large mass and the microparticle to drive the resonator. With this, the gravitational constant could be determined more accurately.

Bibliography

[1] G. S. MacCabe, H. Ren, J. Luo, J. D. Cohen, H. Zhou, A. Sipahigil, M. Mirhosseini, and O. Painter, *Phononic bandgap nano-acoustic cavity with ultralong phonon lifetime*, ArXiv preprint , 1 (2019).

[2] J. D. Teufel, T. Donner, D. Li, J. W. Harlow, M. S. Allman, K. Cicak, A. J. Sirois, J. D. Whittaker, K. W. Lehnert, and R. W. Simmonds, *Sideband cooling of micromechanical motion to the quantum ground state*, Nature **475**, 359 (2011).

[3] R. Abdolvand, B. Bahreyni, J. E. Lee, and F. Nabki, *Micromachined resonators: A review*, Micromachines **7** (2016).

[4] D. Mason, J. Chen, M. Rossi, Y. Tsaturyan, and A. Schliesser, *Continuous force and displacement measurement below the standard quantum limit*, Nature Physics **15**, 745 (2019).

[5] B. van Waarde, *The Lead Zeppelin*, PhD thesis, 2016.

[6] A. Vinante, P. Falferi, G. Gasbarri, A. Setter, C. Timberlake, and H. Ulbricht, *Ultralow mechanical damping with Meissner-levitated ferromagnetic microparticles*, Physical Review Applied **13**, 064027 (2020).

[7] G. R. Fowles and G. L. Cassiday, *Analytical Mechanics, seventh edition, international edition*, (2005).

[8] J. W. Rohlf, *Modern Physics from a to Z0*, (1994).

[9] W. Meissner and R. Ochsenfeld, *Ein neuer Effekt bei Eintritt der Supraleitfähigkeit*, Die Naturwissenschaften **21**, 787 (1933).

[10] F. London and H. London, *The Electromagnetic Equations of a Supraconductor*, The Royal Society **149**, 71 (1935).

[11] A. H. Nayfeh and D. T. Mook, *Nonlinear Oscillations*, page 50 (2008).

[12] O. Usenko, *Development and testing of the gravitational wave antenna MiniGRAIL in its full-featured configuration*, PhD thesis, 2012.

[13] D. J. Griffiths, *Introduction to Electrodynamics, fourth edition, international edition*, (2014).

[14] C. A. Hampel, *The Encyclopedia of the Chemical Elements*, page 256 (1968).

[15] M. de Wit, *Advances in SQUID-detected magnetic resonance force microscopy*, PhD thesis, 2019.

[16] G. Wijts, *Magnetic resonance force microscopy at milliKelvin temperatures*, PhD thesis, 2013.

[17] M. Ortner and L. G. C. Bandeira, *Magpylib: A free Python package for magnetic field computation*, SoftwareX **11**, 100466 (2020).